A Programmable Mechanical Freedom and Variable Stiffness Soft Actuator with Low Melting Point Alloy

Yufei Hao, Tianmiao Wang, and Li Wen[(✉)]

School of Mechanical Engineering and Automation, Beihang University, Beijing, China
liwen@buaa.edu.cn

Abstract. Soft robotic technologies have been widely used in the fields like bio-robotics, wearable devices, and industrial manipulations. However, existing soft robots usually require multiple pneumatic/fluidic channels for pressurizing soft material segments in series or in parallel to achieve multiple mechanical degrees of freedom. In this study, we demonstrated a soft actuator embedded with Low-Melting-Point Alloy (LMPA), with which the mechanical degrees and stiffness can be selectively controlled. The LMPA was embedded in the bottom of the actuator, with the Ni-Cr wires serpentining under different positions of the LMPA layer. Through a reheating- recrystallizing circle, the actuator can self-heal and recover from the crack state. The melting process of the LMPA under different currents and different sections, the variable stiffness, the self-healing properties, and the programmable mechanical freedom of the actuator was explored through experiments. The results showed that the LMPA could be melted about 10 s under the current of 0.7 A. With the LMPA, the bending force and the elasticity modulus of the actuator could be enhanced up to 16 times and 4,000 times separately. Moreover, up to six motion patterns could be achieved under the same air pressure inflated to a typical single-chamber soft actuator. The combination of Low-Melting-Point Alloy and the soft actuators may open up a diversity of applications for future soft robotics.

Keywords: Variable stiffness · Low-Melting-Point alloy · Soft actuator · Programmable mechanical freedom

1 Introduction

Soft robotics, which has promising features such as lightweight, low-cost, easy fabrication and high compliance [1], is a multi-disciplinary research area involving chemistry [2], material science [3], biology [4–8] and mechanics [9]. Soft robotic technologies have been widely used in actuation [10], sensing [11], and the nonlinear dynamics control [12]. Besides, soft robots have been widely studied in the applications like manipulation [13], locomotion [14], wearable devices [15] and invasive surgery [16]. However, there exist two drawbacks that limit the further development of soft robots. The materials of soft actuators are mostly silicon rubbers which has high compliance, however, restrict the capacity of the robots in many applications that require high mechanical strength. Besides, most of the soft actuators only have one kind of motion

pattern when they were in operation [10]. For the dexterous movement, multiple pneu-matic/fluidic channels for pressurizing soft material segments in series or parallel were needed [16, 17].

Recently, to improve the stiffness without diminishing the mobility of the soft robots, several materials with tunable stiffness have been used in soft robotics. For example, the viscosity of the macro-particle of magnetorheological (MR) or electrorheological (ER) fluids could be changed under the stimulus of the electric or magnetic field [18, 19]. However, these materials require external electromagnets or high voltage capacitors and have limited functional times. By packing particles into a membrane, the stiffness could also be changed when a vacuum pressure was exerted, so-called jamming [20, 21]. However, the jamming effect requires much volume to achieve a great stiffness. Shape memory polymer, whose elasticity modulus could be changed if the temperature is above the glass transition temper-ature, was also used for variable stiffness [22]. However, the response is slow due to the poor thermal conductivity of the SMP material. For the change of the mechanical free-doms, shape memory polymer [23], selectively-placed flexible conformal covering [24] or paper-elastomer composites [25] were used. However, the major mechanical property was prescribed during the design and fabrication stage and cannot be changed on working.

Moreover, previous methods of changing stiffness or freedoms have two major drawbacks: (1) the relative stiffness changing is limited; (2) the structure would not recover if they were broken. In contrast, Low-Melting-Point alloys (LMPAs), which can transform from solid state to liquid state by heating are ideal choice to overcome the two problems. The LMPAs have two major advantages: (1) they can increase their elastic stiffness up to several thousand orders [26]; (2) They can heal themselves from crack or external impact by a reheating-recrystallizing process [27]. Recently, researchers started to apply the LMPA to the soft manipulators [28, 29], the metal-elastomer foams [27] and the fibers [30]. However, no study addressed a robotic device that allows the mechanical freedoms and stiffness to be changed simultaneously.

In this article, we demonstrated an LMPA embedded soft actuator with program-mable mechanical freedoms and stiffness. By selectively activating the Ni-Cr wires under the LMPA layer, we can choose which sections of the LMPA layer to be melted. Thermal actuation experiments were conducted to explore the melting process of the LMPA under different currents and the influence of heating one section on the others. To test the stiffness variation and self-healing property of the actuator, we conducted mechanical experiments to measure the bending stiffness and elasticity modulus of the actuator when the LMPA was in the solid state and liquid state separately. Finally, various motion patterns were realized on a soft actuator with a single channel to verify the variable mechanical freedoms.

2   Materials and Methods

2.1   The Design and Fabrication of the Soft Actuator with LMPA

The detailed structure of the LMPA embedded soft actuator is depicted in Fig. 1. Figure 1a shows the prototype and the CAD model of the actuator. The actuator is composed of two parts: the top extensible part and the multilayer bottom part. The top

part is a rippled structure which could make the soft actuator bend in two directions. For the variation of the mechanical freedom and stiffness of the soft actuator, a thin layer of LMPA was embedded into the bottom part of the soft actuator. Ni-Cr wires were used to selectively melt the different sections (section I, II and III) of the LMPA because of the high electrical resistivity of the material. The detailed structure of the multilayer bottom part is shown in Fig. 1b. The structure has three kinds of layers: the LMPA layer, the Ni-Cr wire layer, and the silicon rubber (dragon skin 10, smooth-on Inc., USA) seal layer. The LMPA layer was a 1.2 mm thick rectangular plate with many through holes. Because the LMPA layer has no adhesive force on the silicon rubber, by making many though holes in the LMPA layer, the silicon rubbers above and underneath the LMPA could be connected via the holes. Thus making the structure more compact. The LMPA is a type of alloy with the following composition by weight: 32.5% bismuth, 51% indium, and 16.5% tin. We choose this material for its low melting point which is about 62 °C and the high elasticity modulus. The Ni-Cr wire layer was fabricated by pouring the uncured silicon rubber on the pre-twined Ni-Cr wires with a diameter of 0.1 mm. For
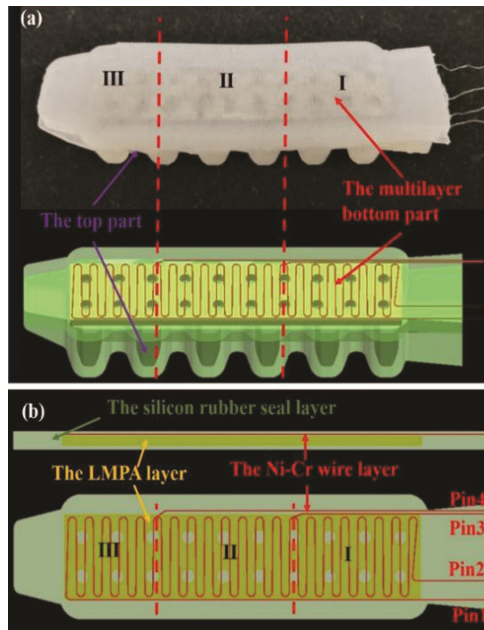

Fig. 1. The design of the soft actuator with variable mechanical freedom and stiffness. (a) The structure composition of the soft actuator. The structure has three mechanical freedoms by heating the different sections (section I, II and III) of LMPA. (b) The detailed structure of the multilayer bottom part of the actuator. The part has three difference layers. By selectively powering any two of the four pins, the corresponding sections of the LMPA layer would be melted: apply currents to pins 1 and 2, the three sections will all be melted; apply currents to pins 1 and 3, the section II and III will be melted; apply currents to pins 1 and 4, the section III will be melted; applying currents to pins 2 and 3, the section I will be melted; apply currents to pins 2 and 4, the section I and II will be melted; apply currents to pins 3 and 4, the section II will be melted.

the aim of selectively melting the three sections of the LMPA layer, two additional wires were separately connected to the middle of the whole Ni-Ci wire. Totally four pins were provided for the power. The total thickness of the layer was 0.7 mm. By applying currents on any two of the four pins, the corresponding LMPA above the surface of the wires should be melted. Thus the mechanical freedom and the stiffness of the actuator could be changed. The silicon rubber layer was used to bond the LMPA layer and the Ni-Cr wire layer together and seal the LMPA layer in an enclosure space.

2.2   The Melting Process Test of the LMPA

Two experiments were conducted to test the thermal conduction behavior of the LMPA. For simplification, only the bottom part was used for the test. The first experiment was to test the temperature ascending process and the melting speed of the LMPA under different currents. For this experiment, the multilayer bottom part was suspended in the air by several wires under the bottom to minimize the heat loss through contact with other media. Four constant electrical currents (0.4 A, 0.5 A, 0.6 A and 0.7 A) were used to melt the whole LMPA layer separately. During each heating process, the surface temperature of the sample was recorded by an infrared imager (Ti400, Fluck Thermography, America). After the heating, it took about 4 min for the sample to return to room temperature before the next heating process. The data was finally addressed by the supporting software (SmartView 4.1, Fluck Thermography, America). When heating only one section of the LMPA, it should be better that the heater will not affect the adjacent segments significantly and the stiffness transform between these segments is smooth and gradient. So the other experiment was designed to test the influence of heating one section of the LMPA on the adjacent sections. For this purpose, only the middle section of the LMPA was heated under the current of 0.5 A. Then the surface temperature of the whole sample was recorded, and the temperature distributions between the adjacent segments were compared for further analysis.

2.3   Bending Stiffness and Elasticity Modulus of the Actuator

When the LMPA is at the solid state, the mechanical property of the soft actuator will be dominated by the rigid LMPA layer, while the silicon rubber structure will be the dominate part when the LMPA is melted. Besides, it can recover its mechanical properties from the crack through a reheating and recrystallizing circle. For the stiffness variation test of the soft actuator, a comparison experiment was conducted to test the bending force of the soft actuator when the LMPA was in actuation and non-actuation state. Besides, we also tested the bending strength of the actuator after several reheating-recrystallizing cycles to verify the healing property of the LMPA. For simplification, only the multilayer bottom part was tested. The experiment setup was illustrated in Fig. 2. The sample was fastened to the fixator. The connector, fixed to the force sensor which was fastened to a robot arm, was used to contact the sample and exert a force on the sample. The lateral distance between the connector and the base of the sample was 25 mm. During the test, the connector first contacted the surface of the sample, then moved downward with a speed of 0.5 mm/s. After moving 2 mm, the connector

suspended 5 s before the next moving. The total displacement was 20 mm for the whole test. During the process, the force date was acquired by a LabVIEW program at a sample rate of 50 Hz. Totally twelve samples were tested for each condition of the LMPA (liquid, solid and cycle test) separately.
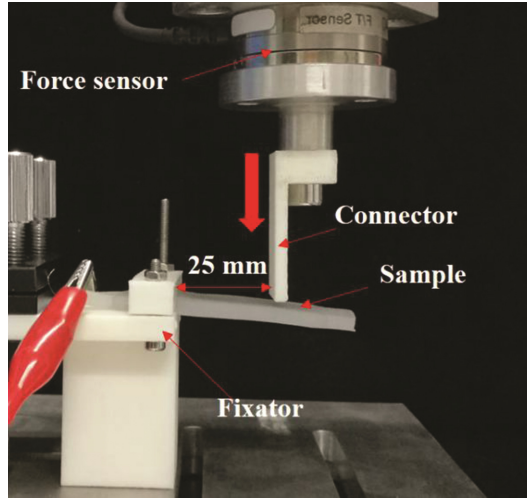

Fig. 2. The experiment setup for the bending stiffness test of the actuator. The sample was fastened to the fixator. The connector was fixed to the robot arm via the force sensor. The lateral distance between the connector and the base of the sample was 25 mm. During the test, the robot arm was moved downward with a speed of 0.5 mm/s and suspended 5 s for each 2 mm displacement.

To verify the elasticity modulus of the LMPA for the self-healing property, we fabricated three bottom part samples for the elasticity modulus measurements before and after the samples were broken. For each sample, we first tested the strain and stress of the LMPA layer; then the strain and stress was tested again after a remelting and refreezing process for the sample. The experiment was conducted on the universal material test machine (exceed model E44, MTS, America). During the test, the sample was fastened by the two clamps of the machine. The initial distance between the two clamps was 30 mm. Then the upper clamp was moved upwards at the speed of 0.5 mm/s until the sample was broken. The force and the displacement values were recorded at the sample rate of 20 Hz.

2.4   Variable Mechanical Freedoms of the Soft Actuator

By applying currents to any two of the four pins, the corresponding sections of the LMPA layer would be melted. Thus the mechanical freedom will be changed. To analysis the motion patterns of the soft actuator when different sections of the LMPA layer were melted, we fixed the actuator to a base, then powered the matched pins according to Fig. 1b to melt the corresponding sections of the LMPA. After the metal was melted,

we inflated the actuators with the pressure up to 30 kPa and captured the motion process of the actuator. Besides the programmable mechanical freedoms, the actuator can sustain its shape under the deflation state after the LMPA was solidified. To verify this property, we first melted the LMPA and inflated the soft actuator to 40 kPa and captured the motion profile of the actuator. Then waited about 5 min for the LMPA to refreeze and deflate the actuator. The profile of the final state was compared with the previous one.

3   Results and Discussion

3.1   The Thermal Behavior of the LMPA

Figure 3 shows the results of the thermal actuation test of the LMPA. As Fig. 3b shows, for all the four currents, the melting process of the LMPA experienced about three stages. For the first stage, the temperature increased to nearly 56 °C at a linear speed, during which the LMPA only absorbed the energy to reach the melting point but kept in the solid state. For the second stage, the temperature kept constant. The LMPA absorbed energy to transform from the solid state to the liquid state. In the final stage, the LMPA was in the liquid state, and the temperature went on increasing. It could also be concluded from Fig. 3b that with a higher current, the melting period of the LMPA would be sharply cut down. When the current was 0.4 A, it took about 28 s for the LMPA to transfer to liquid state from the room temperature. When the current was increased to 0.5 A, the melting time was about 18 s. Increasing the current to 0.7 A, the melting time would be shorted to about 10 s. A simple model could estimate the melting speed for a given LMPA structure:

$$Ri^2t = \mathrm{mc}\Delta T + \mathrm{mL} \tag{1}$$

Where R is the resistance of the heater, i is the current applied to the heater, m is the mass of the metal, c is the specific heat capacity, ΔT is the temperature difference between the room temperature and the melting point and L is the latent heat of the metal. As the model shows, the power of the heater should be enough to melt the metal structure fast. For this purpose, the Ni-Cr wire was used as the heater for its high electrical resistivity, which is about 62.3 times to that of copper. Besides, the melting time with the relation of current was a quadratic function. That is the reason that the melting speed would increase sharply by increasing the current a little.

Through the pictures in the first row of Fig. 3a, we can see that the surface temperature of the LMPA was equally distributed. This demonstrated that the spaces between the helical Ni-Cr wire would not result in the uneven heating of the LMPA, which may lead to some part of the LMPA cannot be melted. The pictures in the second row of Fig. 3a show the infrared images of heating only section II of the LMPA layer, and Fig. 3c shows the temperature distribution of the middle line (depicted in the last image of Fig. 3a) of the LMPA layer. As these results show, the high temperatures only concentrate on section II (the area between the actuated wires), while the temperatures of the unheated sections decreased drastically with the distance from the heating area increasing. This demonstrated that the heat was mostly absorbed by the section II of the

LMPA, then conducted to the adjacent sections in a sharply decreased speed. The sharp temperature distribution variation demonstrates that the adjacent sections have little interactions when heated separately, which guaranteed that the mechanical freedom would keep constant when heated several times.
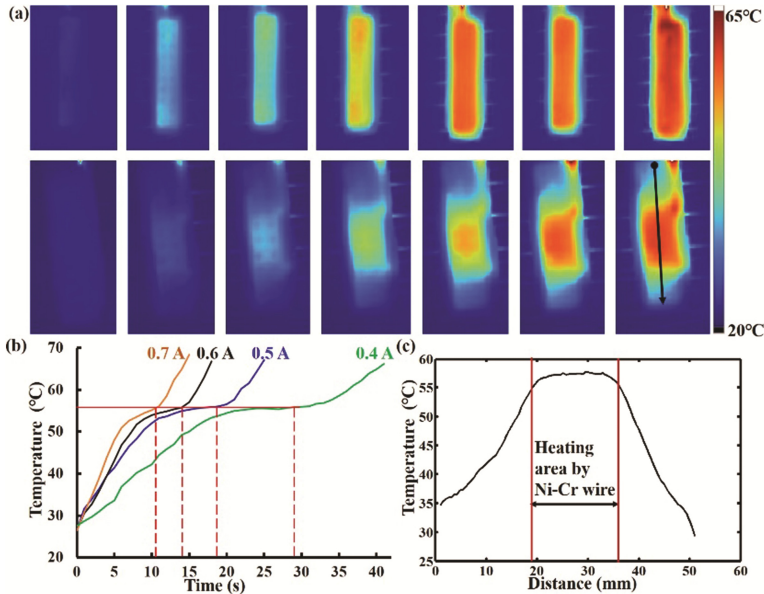

Fig. 3. The thermal behavior of the actuator. (a) The infrared thermal images at different times with the current of 0.4 A. The upper row shows the results of heating the whole LMAP layer, while the lower row shows the results of heating section II of the LMPA layer. (b) The melting process of the LMPA under different currents. As the curves show, the temperature of the LMPA first increased to the melting point, then the LMPA transformed from the solid state to the liquid state with the temperature keeping constant. After that, the temperature went on increasing. (c) The temperature distribution of the middle line of the LMPA when section II was heated. The line and the direction were indicated in the last image of panel b. The red dashed lines show the position of the heating wire. (Color figure online)

3.2   The Variable Stiffness of the Actuator

With the LMPA, the stiffness of the soft actuator could be improved significantly when the metal was at the solid state. However, this rigid structure has little influence on the dexterity of the soft actuator if it was melted. As Fig. 4a shows, the sample even bend downward under the effect of gravity if the LMPA was melted. However, the bending stiffness could be significantly improved when the LMPA was in the solid state. As Fig. 4b shows, the bending force increased linearly with the increasing of the deflection. Besides, the force data is much bigger compared to that when the LMPA was in the liquid state under the same deflection distance. For example, the force of the solid state is about 16 times of that of the liquid state under the deflection of 20 mm, which

demonstrated soundly that the stiffness of the actuator could be significantly enhanced when the LMPA was in the solid state. It could also be deduced that the embedded LMPA could improve the mechanical property of the soft actuator. Furthermore, the soft actuator can recover within 4 min after crack, which could be verified by Fig. 4b and Table 1. As the results show, the bending forces under different heating-cooling cycles were similar under the same deflection. Moreover, the difference between the elasticity modulus of the pre-fractured sample and the same sample after a reheating-refreezing circle is little. This means that the actuator has an excellent self-healing property. The shape, functionality, as well as the mechanical properties of the actuator, could also be restored. These kind of effects are insurmountable by using other variable stiffness materials such as SMP [22] and jamming ground coffee [21]. Besides, the elasticity modulus of the sample could increase about 4,000 times compared to that of the structure without LMPA.
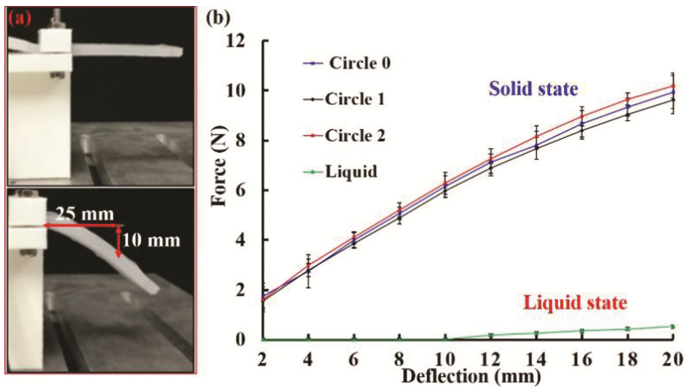

Fig. 4. The results of the bending stiffness test. (a) The real pictures of the sample when the LMPA under the solid state and the liquid state. (b) The force versus deflection of the sample when the LMPA under the solid state and liquid state.

Table 1. The results of the elasticity modulus test of the soft actuator.

Sample state	Elasticity modulus (GPa)	Standard deviation
Pre-fracture	6.12	0.649
Aft-healing	5.92	0.436
Pure rubber	1.5×10^{-4} [31]	–

3.3   The Programmable Mechanical Freedom of the Actuator

By activating the pin matches in Fig. 1b, the corresponding sections of the LMPA layer would be melted, and the mechanical freedom can be changed. This property is well demonstrated in Fig. 5. As the figure shows, the actuator will have various motion patterns under the same pressure if different sections of the LMPA were melted. When pressurized, the un-melted LMPA will restrict the bending so only the melted sections

could bend. This method is more applicable and functional than the fiber-reinforced actuators [15]. By varying the angle of the fiber, the fiber-reinforced actuator can achieve different motion patterns, but these patterns cannot be changed if the structure was finally fabricated. By modifying the motion patterns during work, the actuator will have more application values. For example, it can mimic the variable stiffness bionic structures such as the muscle, and it can contribute to much more grasping strategies if it is used for gripping. Apart from the motion dexterity, the actuator can keep its actuated shape after the LMPA was recrystallized. As Fig. 5b shows, section III of the actuator bent under the pressure of 40 kPa, with large bubbles at the upper rippled part. However, the actuator will keep the same state if the LMPA was solidified, with zero energy consumed. This attribute is very energy-efficient for the long term operations. Such as the long-distance transportation after the gripper grasp the objects.
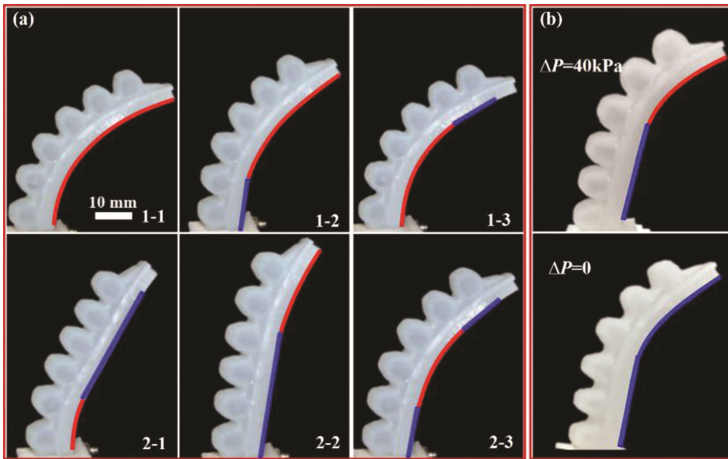

Fig. 5. (a) The various motion patterns of the actuator under the same pressure (30 kPa). "1-1" shows the result by melting the whole LMPA layer; "1-2" shows the result by melting section II and III; "1-3" shows the result by melting section I and II; "2-1" shows the result by melting section I; "2-2" shows the result by melting section III; "2-3" shows the result by melting section II. (b) The shape-retain capability of the actuator. When the LMPA was in solid state (lower picture of panel b), the actuator can still keep the pressurized state (upper picture of panel b) with no additional energy consumption. In all the pictures, the red lines demonstrate that the corresponding sections were melted, while the blue lines show that the relevant sections were solid. (Color figure online)

4 Conclusion

In this paper, a soft actuator with programmable mechanical freedom and variable stiffness was demonstrated. The function of the actuator was achieved by melting different sections of the LMPA layer using the Ni-Cr wires. The thermal experiments showed that the heating method could guarantee the homogeneous temperature distribution, and heating one section of the LMPA layer had little influence on the neighboring sections.

Through mechanical experiments, the self-healing property of the actuator was verified. The bending force of the actuator could increase at least 16 times, and the tensile strength could increase about 13 times owing to the metal. The various motion patterns of the actuator were also studied. By heating different sections of the LMPA layer, the actuator allows for up to 8 motion patterns during working with the same channel under pressurization. Besides, with the LMPA, the actuator can also keep the actuated state with zero power consumptions. The combination of soft robots and LMPA is a promising approach to overcome the drawback of the soft robots, such as the light load capacity, monotonous motions and poor stiffness for some strength needed situations.

References

1. Rus, D., Tolley, M.T.: Design, fabrication and control of soft robots. Nature **521**(7553), 467–475 (2015)
2. Ilievski, F., Mazzeo, A.D., Shepherd, R.F., Chen, X., Whitesides, G.M.: Soft robotics for chemists. Angew. Chem. **123**(8), 1930–1935 (2011)
3. Mac Murray, B.C., An, X., Robinson, S.S., van Meerbeek, I.M., O'Brien, K.W., Zhao, H., Shepherd, R.F.: Poroelastic foams for simple fabrication of complex soft robots. Adv. Mater. **27**(41), 6334–6340 (2015)
4. Lauder, G.V., Wainwright, D.K., Domel, A.G., Weaver, J.C., Wen, L., Bertoldi, K.: Structure, biomimetics, and fluid dynamics of fish skin surfaces. Phys. Rev. Fluids **1**(6), 060502 (2016)
5. Ren, Z., Yang, X., Wang, T., Wen, L.: Hydrodynamics of a robotic fish tail: effects of the caudal peduncle, fin ray motions and the flow speed. Bioinspir. Biomim. **1**(1), 016008 (2016)
6. Wehner, M., Truby, R.L., Fitzgerald, D.J., Mosadegh, B., Whitesides, G.M., Lewis, J.A., Wood, R.J.: An integrated design and fabrication strategy for entirely soft, autonomous robots. Nature **536**(7617), 451–455 (2016)
7. Wen, L., Weaver, J., Lauder, G.: Biomimetic shark skin: design, fabrication and hydrodynamic testing. J. Exp. Biol. **217**(10), 1637–1638 (2014)
8. Wen, L., Weaver, J., Thornycroft, P.M., Lauder, G.: Hydrodynamic function of biomimetic shark skin: effect of denticle pattern and spacing. Bioinspir. Biomim. **10**(6), 066010 (2015)
9. Polygerinos, P., Wang, Z., Overvelde, J.T., Galloway, K.C., Wood, R.J., Bertoldi, K., Walsh, C.J.: Modeling of soft fiber-reinforced bending actuators. IEEE Trans. Rob. **31**(3), 778–789 (2015)
10. Connolly, F., Polygerinos, P., Walsh, C.J., Bertoldi, K.: Mechanical programming of soft actuators by varying fiber angle. Soft Robot. **2**(1), 26–32 (2015)
11. Arabagi, V., Felfoul, O., Gosline, A.H., Wood, R.J., Dupont, P.E.: Biocompatible pressure sensing skins for minimally invasive surgical instruments. IEEE Sens. J. **16**(5), 1294–1303 (2016)
12. Marchese, A.D., Tedrake, R., Rus, D.: Dynamics and trajectory optimization for a soft spatial fluidic elastomer manipulator. Int. J. Robot. Res. **35**(8), 1000–1019 (2015)
13. Hao, Y., Gong, Z., Xie, Z., Guan, S., Yang, X., Ren, Z., Wang, T., Wen, L.: Universal soft pneumatic robotic gripper with variable effective length. In: 35th Chinese Control Conference (CCC), Cheng Du, China, pp. 6109–6114. IEEE (2016)

14. Bartlett, N.W., Tolley, M.T., Overvelde, J.T., Weaver, J.C., Mosadegh, B., Bertoldi, K., Whitesides, G.M., Wood, R.J.: A 3D-printed, functionally graded soft robot powered by combustion. Science **349**(6244), 161–165 (2015)
15. Park, Y.L., Chen, B.R., Young, D., Stirling, L., Wood, R.J., Goldfield, E.C., Nagpal, R.: Design and control of a bio-inspired soft wearable robotic device for ankle-foot rehabilitation. Bioinspir. Biomim. **9**(1), 016007 (2014)
16. Ranzani, T., Gerboni, G., Cianchetti, M., Menciassi, A.: A bioinspired soft manipulator for minimally invasive surgery. Bioinspir. Biomim. **10**(3), 035008 (2015)
17. Gong, Z., Xie, Z., Yang, X., Wang, T., Wen, L.: Design, fabrication and kinematic modeling of a 3D-motion soft robotic arm. In: 2016 IEEE International Conference on Robotics and Biomimetics, Qing Dao, China, pp. 509–514. IEEE (2016)
18. Pettersson, A., Davis, S., Gray, J.O., Dodd, T.J., Ohlsson, T.: Design of a magnetorheological robot gripper for handling of delicate food products with varying shapes. J. Food Eng. **98**(3), 332–338 (2010)
19. Taniguchi, H., Miyake, M., Suzumori, K.: Development of new soft actuator using magnetic intelligent fluids for flexible walking robot. In: 2010 International Conference on Control Automation and Systems (ICCAS), Gyeonggi-do, Korea, pp. 1797–1801 (2010)
20. Wei, Y., Chen, Y., Ren, T., Chen, Q., Yan, C., Yang, Y., Li, Y.: A novel, variable stiffness robotic gripper based on integrated soft actuating and particle jamming. Soft Robot. **3**(3), 134–143 (2016)
21. Wall, V., Deimel, R., Brock, O.: Selective stiffening of soft actuators based on jamming. In: 2015 IEEE International Conference on Robotics and Automation (ICRA), Seattle, USA, pp. 252–257. IEEE (2015)
22. Yang, Y., Chen, Y.: Novel design and 3D printing of variable stiffness robotic fingers based on shape memory polymer. In: 6th IEEE International Conference on Biomedical Robotics and Biomechatronics (BioRob), Singapore, pp. 195–200, June 2016
23. Firouzeh, A., Salerno, M., Paik, J.: Soft pneumatic actuator with adjustable stiffness layers for Multi-DoF actuation. In: 2015 IEEE/RSJ International Conference on Intelligent Robots and Systems (IROS), Hamburg, Germany, pp. 1117–1124. IEEE (2015)
24. Galloway, K.C., Polygerinos, P., Walsh, C.J., et al.: Mechanically programmable bend radius for fiber-reinforced soft actuators. In: 2013 IEEE International Conference on Robotics and Automation, Karlsruhe, Germany, pp. 1–6. IEEE (2013)
25. Martinez, R.V., Fish, C.R., Chen, X., et al.: Elastomeric Origami: programmable paper-elastomer composites as pneumatic actuators. Adv. Funct. Mater. **22**(7), 1376–1384 (2012)
26. Schubert, B.E., Floreano, D.: Variable stiffness material based on rigid low-melting-point-alloy microstructures embedded in soft poly (dimethylsiloxane) (PDMS). RSC Adv. **3**(46), 24671–24679 (2013)
27. Van Meerbeek, I.M., Mac Murray, B.C., Kim, J.W., Robinson, S.S., Zou, P.X., Silberstein, M.N., Shepherd, R.F.: Morphing metal and elastomer bicontinuous foams for reversible stiffness, shape memory, and self-healing soft machines. Adv. Mater. **28**(14), 2801–2806 (2016)
28. Alambeigi, F., Seifabadi, R., Armand, M.: A continuum manipulator with phase changing alloy. In: 2016 IEEE International Conference on Robotics and Automation (ICRA), Stockholm, Sweden, pp. 758–764. IEEE (2016)
29. Zhao, R., Yao, Y., Luo, Y.: Development of a variable stiffness over tube based on low-melting-point-alloy for endoscopic surgery. J. Med. Devices **10**(2), 021002 (2016)
30. Tonazzini, A., Mintchev, S., Schubert, B., Mazzolai, B., Shintake, J., Floreano, D.: Variable stiffness fiber with self-healing capability. Adv. Mater. **28**(46), 10142–10148 (2016)
31. https://www.smooth-on.com/products/dragon-skin-10-medium/. Accessed 21 Apr 2017